Struct Chem (2012) 23:237–243
DOI 10.1007/s11224-011-9857-1

ORIGINAL RESEARCH

Theoretical and computational modelling of functionalization energy for the $C_{6n^2}H_{6n}$ polycyclic aromatic hydrocarbons (PAHs) homologue series

Massimo Fusaro

Received: 5 April 2011 / Accepted: 9 August 2011 / Published online: 27 August 2011

Abstract Based on the free electron metallic disc model, the derivation of a simple expression for evaluation of the Fukui function for the molecular models of polycyclic aromatic hydrocarbons (PAHs) of the general formula $C_{6n^2}H_{6n}$ was described. We also investigated the functionalization energy with OH radicals for the molecular models of PAHs ($n = 1$–6). Our metallic disc model-based functionalization reaction energy was in agreement with the DFT:B3LYP/6-31G(*d*) calculated values. Asymptotic values of the functionalization energies ($n \rightarrow \infty$) were predicted to be -30.1 ± 0.1 and -8.7 ± 0.1 kcal/mol for the external and internal border carbon atoms, respectively.

Keywords Fukui function · PAH · Circumcoronene

Introduction

Polycyclic Aromatic Hydrocarbons [1] (PAHs) are a large family of tarry materials naturally present in, for example, coal and crude oil. In addition, they are also formed in the combustion of all sorts of carbonaceous fuels and hence are found in auto exhaust, cigarette smoke and candle soot. PAHs are known for the persistent detrimental effect of their carcinogenic properties on the environment, due to their long-term stability. PAHs are also the largest known molecules in space [2], and are ubiquitously present with high abundance. Intimately mixed with dust, they are formed in the outflows of evolved and dying stars [3]. They play a vital role in interstellar chemistry and can be used to probe environmental conditions within astronomical objects [2, 3].

A necessary and relatively slow step of many oxidation processes of organic materials is the stable attachment of the hydroxyl radical to the Π electronic system [4]. Hydroxyl radicals are important oxidants in the atmosphere and in the natural waters. Hydroxyl radicals are produced in aqueous solutions via the photolysis of nitrite, nitrate and hydrogen peroxide [5]. Hydroxyl radical-initiated reactions often lead to the formation of mutagenic aromatic compounds, indicating that the health risk assessments of combustion emissions should include atmospheric transformation products [6].

The focus of the present article is a theoretical study on the reaction of hydroxyl radical attachment to the planar conjugated polycyclic aromatic hydrocarbons of the general formula $C_{6n^2}H_{6n}$, $n = 1, 2, 3, 4, 5, 6$ (denoted as S):

$$S + OH^{\bullet} \rightarrow SOH^{\bullet}$$

$SOH^{\bullet}$ is the 'radical' complex, the geometry of which corresponds to the minimum of the potential energy surface. Our former calculations on models systems [7, 8] have shown that the condensed Fukui function [9–11] can be useful in the prediction of the reactivity in silico of highly symmetrical and highly delocalized molecules like nanotubes and fullerenes. A novelty of the present study is the development of a simple model to predict the reactivity of conjugated polycyclic aromatic hydrocarbons of the general formula $C_{6n^2}H_{6n}$ with hydroxyl radicals.

Our research belongs to a long-term project aiming to theoretically predict the reactivity of a broad class of conjugated aromatic hydrocarbons, such as nanotubes and fullerenes.

M. Fusaro (✉)
Faculty of Chemistry, Warsaw University,
Pasteura 1, 02-093 Warsaw, Poland
e-mail: massimo@tiger.chem.uw.edu.pl

Theoretical background

Fukui function

It is known that [9] the Fukui function is a powerful tool to predict the reactivity sites of a molecule.

The Fukui function $f(\underline{r})$ [9–11] is defined as a derivative of electronic density $\rho(\underline{r})$ versus number of electrons N at a constant external potential $v(\underline{r})$ (fixed nuclei):

$$f(\underline{r}) = \left(\frac{\partial \rho(\underline{r})}{\partial N}\right)_{v(\underline{r})} \tag{1}$$

In general, one application of Fukui function is based on the following consideration:

'Of the two different sites with generally similar dispositions for reacting with a given reagent, the reagent prefers the one which is associated with the maximum response of the system's chemical potential. Thus, the greater the Fukui function value, the higher should be the reactivity' [12].

Fukui function for models of the $C_{6n^2}H_{6n}$ PAH homologue series

We studied models of PAHs of the general formula $C_{6n^2}H_{6n}$, Fig. 1.

Metallic disc approximation

In order to evaluate the Fukui function, we approximated our PAH model ($C_{6n^2}H_{6n}$) as a metallic disc of radius R, $R = (3n+1)\frac{a_{cc}}{2}$, Fig. 1. The radius R of the disc was chosen in order to keep in mind the real extension of the electronic density, longer by a_{cc} than the most distant carbon atom from the geometrical center of our S model.

Laplace equation and surface charge density

The Laplacian operator is used for cylindrical coordinates [13]. Keeping in mind that our charged disc model is independent of the azimuthal cylindrical coordinate it follows:

$$\nabla^2\varphi(z,r) = \frac{1}{r}\frac{\partial}{\partial r}\left(\frac{\partial\varphi(z,r)r}{\partial r}\right) + \frac{\partial^2\varphi(z,r)}{\partial z^2} = 0 \tag{2}$$

where the disc symmetry axis is along the z vertical cylindrical coordinate and $\varphi(z, r)$ is the potential of the electrical field.

By solving the partial differential eq. 2 using the standard technique of the variable separation, it follows:

$$\varphi(z,r) = f(r)g(z) \tag{3}$$

Replacing eq. 3 in eq. 2 it follows:

$$\frac{d^2f(r)}{dr^2}r^2 + \frac{df(r)}{dr}r + \lambda^2 f(r)r^2 = 0 \tag{4}$$

$$\frac{d^2g(z)}{dz^2} - \lambda^2 f(z) = 0 \tag{5}$$

The choice of the constant λ^2 (positive number) is because the electrical potential $\varphi(z, r)$ should tend to zero as $|z|$ approaches infinity.

The solution of the differential equations 4 and 5 can be expressed as:

$$f(r) = c_1 J_0(\lambda r) + c_2 Y_0(\lambda r) \tag{6}$$

$$f(z) = c_3 e^{\lambda z} + c_4 e^{-\lambda z} \tag{7}$$

where c_1, c_2, c_3, c_4 are the λ dependent coefficients of the linear combination, and $J_0(\lambda r)$, $Y_0(\lambda r)$ are the Bessel

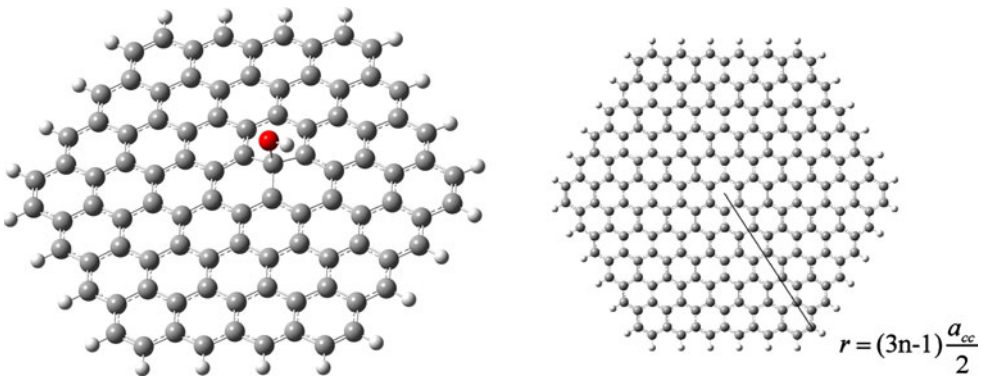

Fig. 1 Typical geometry of a reaction center in SOH$^{\bullet}$ (*left*). S is the molecular model of circumcircumcoronene ($C_{96}H_{24}$, $n = 4$, *right*). The carbon atoms of our planar substrate S ($C_{6n^2}H_{6n}$) are at distance r from the geometric center of the molecule, with $r_k = k\frac{a_{cc}}{2}$ ($k \in [2, 3n\text{-}1]$ and $k \neq 3s$ with k, s integer, $a_{cc} = 1.42$ Å the carbon–carbon bond length). The reacting carbon atom is in this case the internal carbon atom ($k = 2$)

functions of the first kind of order zero and the Bessel functions of the second kind of order zero (also called Weber or Neumann functions), respectively.

From eqs. 3, 6, 7 it follows:

$$\varphi_\lambda(z,r) = (c_1 J_0(\lambda r) + c_2 Y_0(\lambda r))\left(c_3 e^{\lambda z} + c_4 e^{-\lambda z}\right) \quad (8)$$

Boundary conditions

The electrical potential $\varphi(z, r)$is bound and should tend to zero as $|z|$ approaches infinity.

Remembering that $Y_0(\lambda r)$is unbound for $r = 0$ from eq. 8 it follows:

$$\varphi_\lambda(z,r) = c(\lambda) J_0(\lambda r) e^{-\lambda|z|} \text{ with } \lambda > 0 \quad (9)$$

where c is a coefficient.

As the Laplace eq. 2 is a linear equation in $\varphi_\lambda(z, r)$, it follows that a linear combination of eq. 9 is a solution of eq. 2:

$$\varphi(z,r) = \int_0^\infty c(\lambda) J_0(\lambda r) e^{-\lambda|z|} d\lambda \quad (10)$$

We also imposed the following boundary conditions:

$$\varphi(0,r) = V_0 = \int_0^\infty c(\lambda) J_0(\lambda r) d\lambda \text{ with } r \le R \quad (11)$$

i.e. a constant potential V_0 on the metallic disc and

$$\left.\frac{d\varphi(z,r)}{dz}\right|_{z=0} = 0 = \int_0^\infty \lambda c(\lambda) J_0(\lambda r) d\lambda \text{ with } r > R \quad (12)$$

zero electrical field outside the disc ($r > R$) on the plane containing the metallic disc ($z = 0$) for symmetry.

Equations 11 and 12 are *dual integral equations* for $c(\lambda)$.

The general theory of dual integral equations is complicated and not highly developed, but in this case can be solved remembering that:

$$\int_0^\infty \frac{\sin \lambda R}{\lambda} J_0(\lambda r) d\lambda = \begin{cases} \frac{\pi}{2} & r \le R \\ sin^{-1}\left(\frac{R}{r}\right) & r > R \end{cases} \quad (13)$$

and

$$\int_0^\infty \sin(\lambda R) J_0(\lambda r) d\lambda = \begin{cases} \frac{1}{\sqrt{R^2 - r^2}} & r \le R \\ 0 & r > R \end{cases} \quad (14)$$

From eqs. 10–14 it follows:

$$\varphi(z,r) = \frac{2V_0}{\pi} \int_0^\infty \frac{\sin \lambda R}{\lambda} J_0(\lambda r) e^{-\lambda|z|} d\lambda \quad (15)$$

Surface charge density

In our metallic disc model, the electrical field $\underline{E}$ is normal to the surface of the disc, i.e. along the z vertical cylindrical coordinate. Therefore, it follows:

$$\underline{E} = -\underline{\nabla}\varphi(z,r) \quad (16)$$

$$-\left.\frac{\partial\varphi(z,r)}{\partial z}\right|_{z=0} = \frac{\sigma(r)}{\varepsilon_0} \quad (17)$$

where $\sigma(r)$is the surface charge density and ε_0 is the dielectric constant of a vacuum.

From eqs. 14, 15, 17 it follows:

$$\sigma(r) = -\varepsilon_0 \left.\frac{\partial\varphi(z,r)}{\partial z}\right|_{z=0} = \frac{2V_0\varepsilon_0}{\pi} \int_0^\infty \sin(\lambda R) J_0(\lambda r) d\lambda = \frac{2V_0\varepsilon_0}{\pi\sqrt{R^2 - r^2}} \quad (18)$$

The charge q on one face of the disc can be obtained integrating the surface charge density $\sigma(r)$ over one face of the disc, it follows:

$$q = \int_0^R 2\pi r\sigma(r) dr = 4V_0\varepsilon_0 \int_0^R \frac{r}{\sqrt{R^2 - r^2}} dr = 4V_0\varepsilon_0 R \quad (19)$$

From eqs. 18, 19 it follows:

$$\sigma(r) = \frac{q}{2\pi R\sqrt{R^2 - r^2}} \quad (20)$$

Fukui function in 'electrostatic approximation'

In our simplified model, we approximate the electronic density $\rho(\underline{r})$ with the surface charge density $\sigma(r)$. From eqs. 1, 20 it follows:

$$f(r) = \left(\frac{\partial\rho(r)}{\partial N}\right)_{v(\underline{r})} = \frac{\partial\sigma(r)}{\partial q} = \frac{1}{2\pi R\sqrt{R^2 - r^2}} \quad (21)$$

Remembering that in our approximation $\rho(r) \cdot e^- = \sigma(r)$ and $N \cdot e^- = q$ with e^- as the electronic charge.

Replacing in eq. 21 the expression of the radius r, R (Fig. 1), it follows:

$$f(r_k) = f\left(k\frac{a_{cc}}{2}\right) = \frac{2}{\pi a_{cc}^2 (3n+1)\sqrt{(3n+1)^2 - k^2}} = \frac{2}{\pi a_{cc}^2} f(k,n) \quad (22)$$

Reactivity

The focus of the present article is the reaction of hydroxyl radical attachment to the Π electronic system of substrate S.

Assuming that the reaction energy ΔE:

$$\Delta E = \mathrm{E([SOH]^{\bullet})} - \mathrm{E(S)} - \mathrm{E(OH^{\bullet})} \quad (23)$$

is a function of the Fukui function $f(r)$ of the reacting carbon, i.e. is a function of $f(k,n)$ (eq. 22) it follows:

$$\Delta E = a + bf(k,n) \quad (24)$$

Computational methods

We used a quantum mechanical approach, in particular the hybrid Density Functional B3LYP method with a split valence basis set and d polarisation functions 6-31G(d) [14]. This computational model is a reasonable compromise between accuracy and computational cost for isolated systems energy calculations [15].

We performed DFT:B3LYP/6-31G(d) calculations using Gaussian 03 software [16] for molecular models of PAHs ($C_{6n^2}H_{6n}$), and DFT:B3LYP/6-31G(d) for the DFT based periodical model of graphene using the Crystal 03 software [17]. We studied PAH molecular models with the general formula $C_{6n^2}H_{6n}$, $n = 1, 2, 3, 4, 5, 6$ (Fig. 1) and a periodical model of graphene (Fig. 2).

Results

Here, we present results for graphene, then six results for PAH models and finally the estimation of the PAH HOMO-LUMO electronic gaps.

Reaction energy for a periodical model of graphene

We investigated the reaction energy: $\Delta E = \mathrm{E([SOH]^{\bullet})} - \mathrm{E(S)} - \mathrm{E(OH^{\bullet})}$ (Table 1), for three periodical models of graphene:

the periodical model in a double 2D super cell (sc = 2, eight carbon atoms per elementary cell), a triple 2D super cell (sc = 3, 36 carbon atoms per elementary cell) and the periodical model in a quadruple 2D super cell (sc = 4, 64 carbon atoms per elementary cell, Fig. 2). We also calculated the interaction energy E_{intOH} between OH groups for all periodical models (Table 1).

We fitted a linear function of $-(\Delta E - E_{\mathrm{intOH}})$ versus $1/\mathrm{sc}^2$ (Fig. 3), with $1/\mathrm{sc}^2$ proportional to the condensed Fukui function, per elementary cell, calculated in the hypothesis of symmetrical substrate [3] (all the carbon atoms of the periodical graphene are equivalent for symmetry).

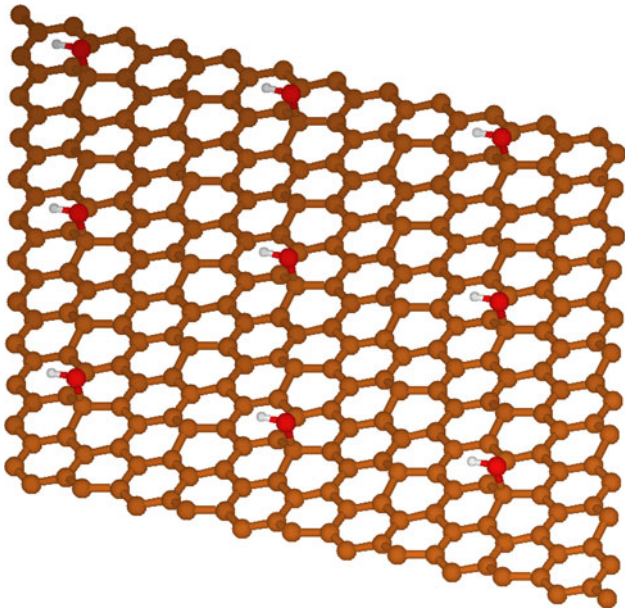

Fig. 2 Periodical model of graphene substrate S, which has reacted with $OH^{\bullet}$ radicals. The periodical model in the picture is composed of nine elementary cells. The calculation for the model in the figure was done in 2D quadruple super cell (sc = 4, 64 carbon atoms per elementary cell); there is only one OH group per elementary cell. The DFT:B3LYP/6-31G(d) calculated reaction energy $\Delta E = \mathrm{E([SOH]^{\bullet})} - \mathrm{E(S)} - \mathrm{E(OH^{\bullet})}$per elementary cell (in this picture quadruple super cell) was corrected subtracting the interaction energy between the OH radicals. It is worth noting that the number of carbon atoms per elementary cell is: $4\mathrm{sc}^2$

From Fig. 3, it can be seen that the energy $(\Delta E - E_{\mathrm{intOH}})$ fits linearly versus $1/\mathrm{sc}^2$ fairly well ($R = 0.99$). From the linear fitting $(\Delta E - E_{\mathrm{intOH}}) = A + \frac{B}{\mathrm{sc}^2}$ (Fig. 3), it follows the reaction energy for a graphene model with one $OH^{\bullet}$, $\Delta E_{\mathrm{graphene}}$.

$$\Delta E_{\mathrm{graphene}} = \lim_{\mathrm{sc}\to\infty}(\Delta E - E_{\mathrm{intOH}}) = \lim_{\mathrm{sc}\to\infty} A + \frac{B}{\mathrm{sc}^2} = A = -15.1 \pm 0.1 \ \mathrm{kcal/mol} \quad (25)$$

This value is in agreement with the value reported in the literature [18] (−15.2 kcal/mol for P3X3) for a model of graphene. It is worth noting that the interaction energy

Table 1 The reaction energy$\Delta E = \mathrm{E([SOH]^{\bullet})} - \mathrm{E(S)} - \mathrm{E(OH^{\bullet})}$, per elementary cell in kcal/mol, B3LYP/6-31G(d) for the periodical models of graphene substrates S (see for example $\mathrm{SOH}^{\bullet}$ sc = 4, Fig. 2)

Super cell sc	ΔE kcal/mol	$E_{\mathrm{int\,OH}}$ kcal/mol	$-\Delta E + E_{\mathrm{int\,OH}}$ kcal/mol
2	−16.6	−0.4	16.2
3	−15.7	0.0	15.7
4	−15.3	0.0	15.3

The interaction energy, E_{intOH} between the OH groups in kcal/mol and $-(\Delta E - E_{\mathrm{intOH}})$ also in kcal/mol

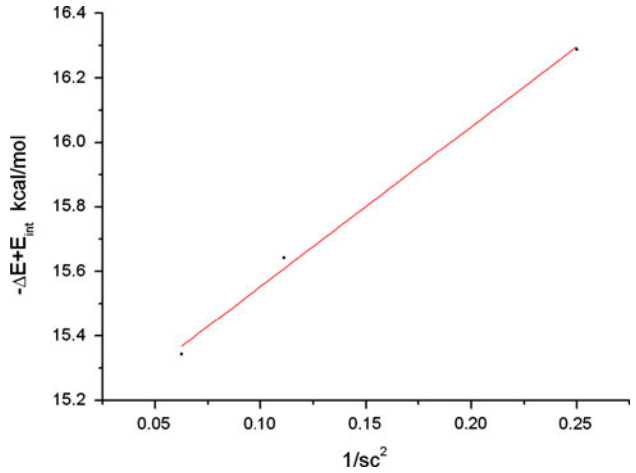

Fig. 3 The DFT:B3LYP 6-31G(d) $-(\Delta E - E_{\text{intOH}})$ energy, fitted using equation: $(\Delta E - E_{\text{intOH}}) = A + \frac{B}{\text{sc}^2}$, $A = -15.1 \pm 0.1$ kcal/mol, $B = -5.0 \pm 0.3$ kcal/mol, $R = 0.99$ (the correlation coefficient)

between OH groups tends to zero when the number of super cells of the periodical models tends to infinity.

Reaction energy for PAH molecular models

We obtained the reaction energy in a broad interval from 2 to 29 kcal/mol (Table 2). We fitted, using eq. 24 the reaction energy: $\Delta E = \text{E}([\text{SOH}]^\bullet) - \text{E(S)} - \text{E}(\text{OH}^\bullet)$ for different reacting carbon atoms k (Table 3) versus $f(k,\text{n})$(eqs. 22, 24), see Figs. 4 and 5.

For the most internal reacting carbon atoms ($k = 2$, Fig. 1), $f(k,\text{n})$ (eq. 22), in this case, and for $n > 1$,$f(2,\text{n})$ can be approximated with the expression:

$$f(2,n) \approx \frac{1}{(3n+1)^2} \tag{26}$$

For the external border reacting carbon atoms ($k = 3n - 1$), $f(k,\text{n})$ (eq. 22), in this case, $f(3\text{n} - 1,\text{n})$ can be replaced with the expression:

$$f(3n-1,n) = \frac{1}{(3n+1)\sqrt{(12n)}} \tag{27}$$

The results are in good agreement with the theoretical eq. 24. For the external border reacting carbon atoms ($k = 3n - 1$), eq. 24 has been expanded adding a parabolic term ($\Delta E = a + bf(k,n) + df(k,n)^2$).

It is worth noting that the limit for n that tends to infinity of the reaction energy ΔE is: $\lim_{n\to\infty}\Delta E = a$ i.e. -8.7 ± 0.1 kcal/mol for the internal reacting carbon atoms ($k = 2$, Fig. 4) and $a = -30.1 \pm 0.1$ kcal/mol for the external border carbon atoms ($k = 3n - 1$, Fig. 5). In the case $k = 2$, the value of -8.7 ± 0.1 kcal/mol is different from the one of graphene, -15.1 ± 0.1 kcal/mol (eq. 25). This fact can be explained by keeping in mind that in our molecular model of substrate S, the external border atoms are hydrogen atoms. These atoms tend to be infinitely far from the reacting carbon atoms ($k = 2$), in the limit for n that tends to infinity. The number of border hydrogen atoms

Table 2 The reaction energy $-\Delta E$, in kcal/mol, B3LYP/6-31G(d) for different $C_{6n^2}H_{6n}$ substrates S (see for example $SOH^\bullet$ $n = 4$, $k = 2$ Fig. 1) and different reacting carbon atoms k ($k = 2$ corresponds to the most internal carbon atoms (Fig. 1), while $k = 3n - 1$ are the external border carbon atoms

n	Name	$-\Delta E$ kcal/mol $k = 2$	$-\Delta E$ kcal/mol $k = 3n - 1$
1	Benzene		15.3
2	Coronene	2.6	21.9
3	Circumcoronene	5.7	24.6
4	$(\text{circum})_2$coronene	6.9	26.2
5	$(\text{circum})_3$coronene	7.6	27.4
6	$(\text{circum})_4$coronene		28.4

Table 3 The DFT:B3LYP/6-31G(d) calculated HOMO-LUMO gap E_{gap} (eV) versus n of our $C_{6n^2}H_{6n}$ molecular model of the substrate S

E_{gap} eV	n
7.7	1
4.0	2
2.8	3
2.1	4
1.6	5
1.3	6

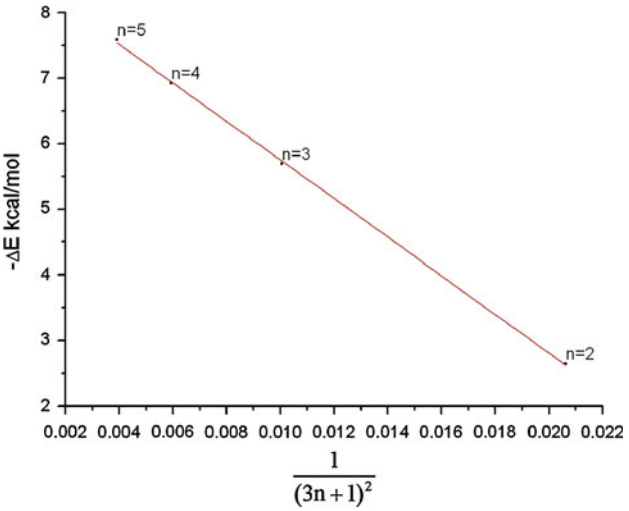

Fig. 4 The DFT:B3LYP/6-31G(d) reaction energy $\Delta E = \text{E}([\text{SOH}]^\bullet) - \text{E(S)} - \text{E}(\text{OH}^\bullet)$ for the $k = 2$ (Fig. 1) $C_{6n^2}H_{6n}$ model of the substrate S versus $\frac{1}{(3n+1)^2}$, fitted using the linear equation: $\Delta E = a + \frac{b}{(3n+1)^2}$, $a = -8.7 \pm 0.1$ kcal/mol (asymptotic value for the internal border carbon atoms), $b = 294 \pm 4$, $R = 0.99$ (the correlation coefficient)

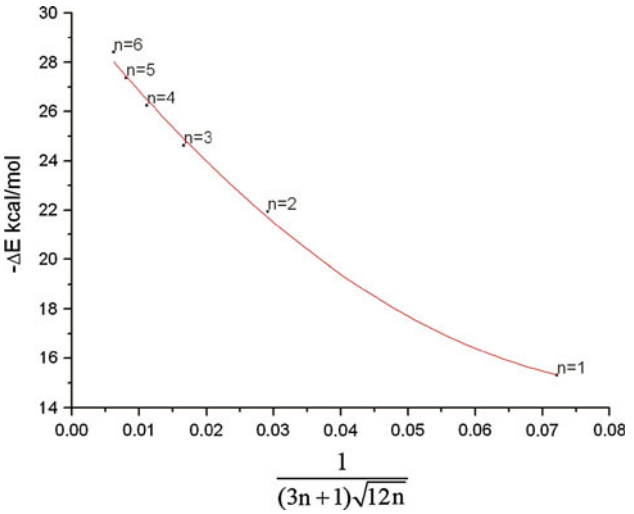

Fig. 5 The DFT:B3LYP/6-31G(*d*) reaction energy $\Delta E = E([SOH]^{\bullet}) - E(S) - E(OH^{\bullet})$ for the $k = 3n - 1$ $C_{6n^2}H_{6n}$ model of substrate S versus $\frac{1}{(3n+1)\sqrt{(12n)}}$, fitted using the parabolic equation: $\Delta E = a + \frac{b}{(3n+1)\sqrt{(12n)}} + \frac{d}{((3n+1)\sqrt{(12n)^2}}$, $a = -30.1 \pm 0.1$ kcal/mol (asymptotic value for the external border carbon atoms), $R = 0.99$ (the correlation coefficient)

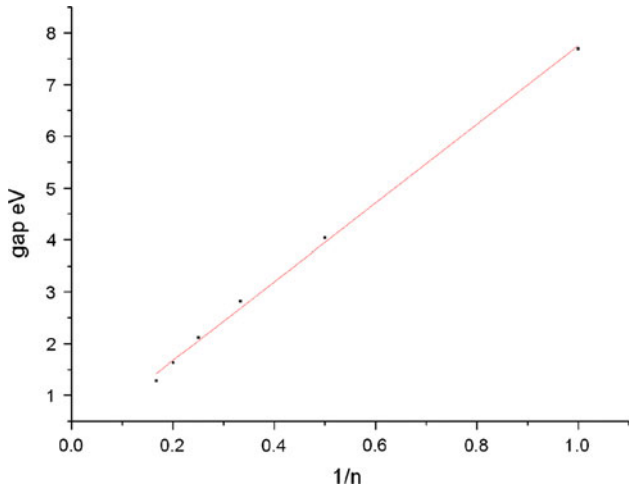

Fig. 6 Linear fit of the DFT:B3LYP/6-31G(*d*) calculated HOMO-LUMO gap E_{gap} (eV) versus $1/n$ (Table 3) using the equation $E_{gap} = E_{gap\,n\to\infty} + \frac{\beta}{n}$, $E_{gap\,n\to\infty} = 0.2 \pm 0.1$ eV, $\beta = 7.6 \pm 0.2$ eV, $R = 0.99$ (the correlation coefficient)

tends also to infinity ($C_{6n^2}H_{6n}$) in the limit for n that tends to infinity. These two opposite effects can cancel each other out, giving a finite contribution to the reaction energy and explaining the different values obtained for graphene.

HOMO-LUMO electronic gap

We also calculated the DFT:B3LYP/6-31G(*d*) calculated HOMO-LUMO gap E_{gap} for our $C_{6n^2}H_{6n}$ molecular model of substrate S. The results are shown in Table 3. We fitted using the linear equation $E_{gap} = E_{gap\,n\to\infty} + \frac{\beta}{n}$ to the DFT:B3LYP/6-31G(*d*) calculated HOMO-LUMO gap (Fig. 6). The electronic gap for our $C_{6n^2}H_{6n}$ molecular model of substrate S (Fig. 6) linearly decreased versus $1/n$, becoming a small gap semiconductor ($E_{gap\,n\to\infty} = 0.2 \pm 0.1$ eV, Fig. 6), which was consistent with our metallic disc model.

Conclusions

In all the investigated $C_{6n^2}H_{6n}$ molecular models, the prediction of energies based on the simple formulas derived on the basis of a metallic disc are in good agreement with the quantum mechanical DFT:B3LYP/6-31G(*d*) ($n = 1$–6). Asymptotic values of the functionalization energies ($n \to \infty$) as predicted from the present simple theory were -30.1 ± 0.1 and -8.7 ± 0.1 kcal/mol for the external and internal border carbon atoms, respectively.

Acknowledgements The Interdisciplinary Center of Mathematical and Computational Modelling (ICM) of Warsaw University is acknowledged for computer time and facilities within the G18-6 computer grant. Prof. A. Leś is acknowledged for reading and commenting on the article.

References

1. Harvey RG (1991) Polycyclic aromatic hydrocarbons. Cambridge University Press, Cambridge
2. Pathak A, Rastogi S (2007) Spectrochim Acta A 67:898–909
3. Won DE, Park JY (2004) Astrophys J 607:342–345
4. Savage NH, Harrison RM, Monks PS, Salisbury G (2001) Atmos Environ 35:515–524
5. Kahan TF, Zhao R, Donaldson DJ (2010) Atmos Chem Phys 10:843–854
6. Atkinson R, Arey J (1994) Environ Health Perspect 102:117–125
7. Fusaro M (2010) J Comput Theor Nanosci 7:2393–2400
8. Fusaro M (2009) J Comput Theor Nanosci 5:1175–1180
9. Mondal P, Hazarika KK, Deka RC (2003) PhysChemComm 6:24–27
10. Chandra AK, Nguyen MT (2002) Int J Mol Sci 3:310–323
11. Chermette H (1999) J Comp Chem 20:129–154
12. Parr RG, Yang WJ (1984) Am Chem Soc 106:4049–4050
13. Jackson JD (1975) Classical electrodynamics, 2nd edn. John Wiley & Sons, New York
14. Hehre WJ, Random L, Schleyer PVR, Pople JA (1987) Ab initio molecular orbital theory. Wiley, New York
15. Yates BF (2002) Annu Rep Prog Chem B 98:607–638
16. Gaussian 09, Revision A.02, Frisch MJ, Trucks GW, Schlegel HB, Scuseria GE, Robb MA, Cheeseman JR, Scalmani G, Barone V, Mennucci B, Petersson GA, Nakatsuji H, Caricato M, Li X,

Hratchian HP, Izmaylov AF, Bloino J, Zheng G, Sonnenberg JL, Hada M, Ehara M, Toyota K, Fukuda R, Hasegawa J, Ishida M, Nakajima T, Honda Y, Kitao O, Nakai H, Vreven T, Montgomery JA, Jr., Peralta JE, Ogliaro F, Bearpark M, Heyd JJ, Brothers E, Kudin KN, Staroverov VN, Kobayashi R, Normand J, Raghavachari K, Rendell A, Burant JC, Iyengar SS, Tomasi J, Cossi M, Rega N, Millam JM, Klene M, Knox JE, Cross JB, Bakken V, Adamo C, Jaramillo J, Gomperts R, Stratmann RE, Yazyev O, Austin AJ, Cammi R, Pomelli C, Ochterski JW, Martin RL, Morokuma K, Zakrzewski VG, Voth GA, Salvador P, Dannenberg JJ, Dapprich S, Daniels AD, Farkas O, Foresman JB, Ortiz JV, Cioslowski J, Fox DJ (2009) Gaussian, Inc., Wallingford CT

17. Saunders VR, Dovesi R, Roetti C, Orlando R, Zicovich-Wilson CM, Harrison NM, Doll K, Civalleri B, Bush IJ, D′Arco P, Llunell M (2003) Crystal03 Universita‘ di Torino. Torino, Italy
18. Ghigo G, Maranzana A, Tonachini G, Zicovich-Wilson CM, Causà M (2004) J. Phys Chem B 108:3215–3223